An Extension of the Linear Embedding via Green's Operators Method for the Analysis of Disconnected Finite Antenna Arrays

Salman Mokhlespour[*]**, Vito Lancellotti, and Anton G. Tijhuis**

Abstract—We describe an extension of the linear embedding via Green's operators (LEGO) method to the solution of finite antenna arrays comprised of disconnected elements in a homogeneous medium. The ultimate goal is the calculation of the admittance matrix and the radiation pattern of the array. As the basic idea is the inclusion of an array element inside an electromagnetic "brick," the first step towards the solution consists of the definition and numerical calculation of hybrid scattering-admittance operators which extend the notion of scattering operators of equivalent currents introduced in the past. Next, the bricks are combined by means of the usual transfer operators to account for the multiple scattering between the bricks. Finally, LEGO is complemented with the eigencurrents expansion so as to reduce the size of the problem. With the aid of a numerical example we discuss the validation of the approach and the scaling of the total CPU time as a function of the elements forming the array.

1. INTRODUCTION

The solution of radiation problems involving large antenna arrays is not as a computationally intensive task. When the array in question spans many wavelengths in one or more spatial dimensions, perhaps the structure can be assumed as infinite and periodic [1, 2], and the analysis is then restricted to a suitable fundamental cell. However, if the periodic approximation is not quite justified and dedicated solution strategies are not adopted, the calculation time and memory requirements may easily make it impractical to analyze many configurations in a design process.

To overcome this limitation, many numerical methods have been proposed, which allow analyzing finite antenna arrays accurately and efficiently. For instance, if the elements are arranged in a regular pattern, the "windowing" of the relevant periodic Green's function has been used to account for edge effects [3]. Other approaches, such as the synthetic functions [4], the characteristic basis functions [5] and the eigencurrents [6] employ aggregate or macro basis functions (MBFs) to reduce the degrees of freedom (DoF) and, ultimately, the simulation time. These strategies are quite general in that they can handle, in principle, antenna arrays in which the positions of the elements do not follow a repetitive pattern. By contrast, domain decomposition methods (DDMs), such as the equivalence principle algorithm [7], are based on the initial conceptual separation of the problem into sub-domains, each one enclosing an array element. The sub-domains are first characterized independently; this is a relatively fast procedure, so long as sub-domains can be defined smaller than or comparable to the wavelength. The mutual coupling between the elements is then *exactly* included in the formulation, when the sub-domains are combined together as prescribed by the geometry of the array. In practice, both MBFs and DDMs aim at compressing the weak form of the original functional equations; the reduced matrices are generally better conditioned and, more importantly, amenable to inversion with direct methods. Furthermore, with DDMs fine geometrical details and related strong local interactions are handled separately from the distant weak interactions, and this feature enables the efficient treatment of multi-scale structures.

For all these reasons, we deem it profitable to extend the linear embedding via Green's operators (LEGO) method [8, 9] to the solution of finite antenna arrays comprised of disconnected metallic elements in a homogeneous medium. In short, LEGO is a DDM that has been applied to both 2-D [8] and 3-D [9] electromagnetic (EM) scattering from clusters of objects; the interaction between a metallic antenna and a set of bodies (e.g., plasma discharges) has also been tackled successfully with LEGO [10, 11]. However, formulating the radiation from finite antenna arrays calls for a substantial overhaul of the approach, and the resultant upgraded LEGO constitutes the topic and the novelty of this paper, as compared to previous work [9, 10, 12, 13].

In the standard LEGO, the separation into sub-domains is realized by enclosing one or more bodies inside an EM "brick." When the independent sources are located outside a brick[†] [9, Fig. 1], the latter can be described by means of a scattering operator that links equivalent incident currents to equivalent scattered currents. Hence, to apply the LEGO method to antenna arrays it seems natural to include each array element inside a brick, which we then characterize by means of a hybrid *scattering-admittance* operator [14], that is, a map between impressed quantities (incident currents on the brick's boundary and voltage generator at the antenna port) and secondary quantities (scattered currents on the brick's boundary and electric current at the antenna port). As a result, we can formulate an array problem by combining bricks as usual, but to accommodate for the scattering-admittance operators, we must write a new set of LEGO equations (cf. [9, Eqn. (16)]). The weak form of the latter can be compressed with the eigencurrents, i.e., MBFs defined on the boundary of a brick, as done in [9, Section IV].
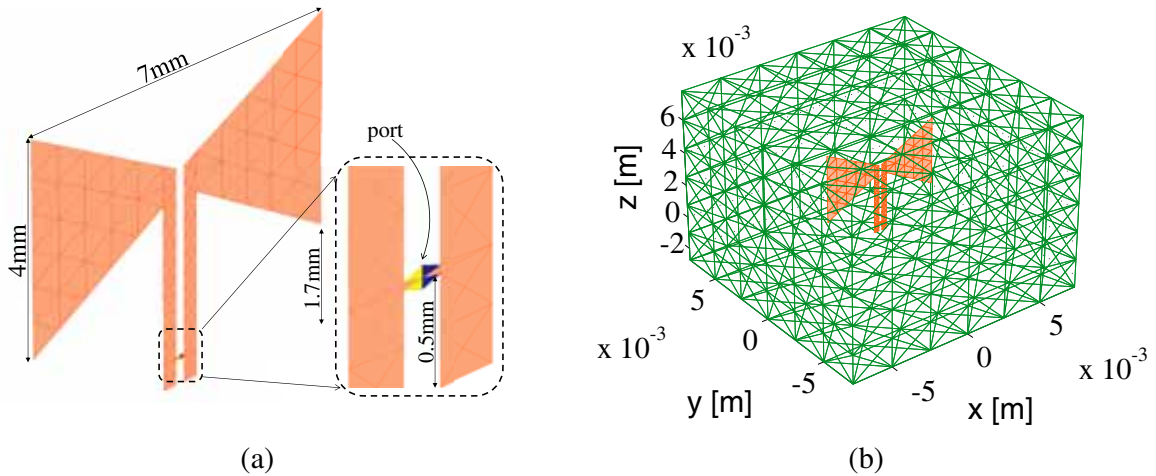

Figure 1. LEGO for antenna arrays: (a) close-up of a bow-tie antenna showing the triangular-faceted mesh and the port region; (b) the same bow-tie antenna enclosed in a cuboidal brick.

At the cost of a little computational overhead (namely, the calculation of the scattering-admittance operators) solving an array with LEGO is advantageous for the following reasons:

(i) Since the scattering-admittance operator depends only on the shape of the enclosed antenna and of the surrounding brick, arrays with different number of elements and, possibly, different spatial arrangements can be efficiently modelled and solved by conceptually combining a set of bricks.

(ii) Since the scattering-admittance operator is designed to provide access to the antenna port within a brick, lumped elements connected to the port can be easily included in the relevant equations.

(iii) Since non-uniform meshes (see Fig. 1(a)) are needed to model fine geometrical details, the very separation of the geometry into bricks likely leads to a better conditioned algebraic system, as the mesh of the bricks' boundaries can be made uniform (see Fig. 1(b)).

(iv) Since the size of said algebraic system can be reduced by using few dominant eigencurrents, solving the array requires inverting a comparatively small matrix, which can be done with direct solvers.

[†] The occurrence of elemental electric or magnetic dipoles within a brick can be handled by augmenting the scattered currents with a "generator" term that accounts for the fields radiated by the independent sources [12].

Admittedly, real-life arrays comprised of metallic and dielectric parts and elements connected by current-carrying conductors (cf. [7]) may not fit in the LEGO framework to be described below. Still, accounting for all details is hardly necessary in a preliminary analysis, as the main features of the radiation pattern (RP) can likely be captured with a simplified antenna model. Therefore, LEGO for disconnected arrays can be beneficial, e.g., for the fast determination of the RP of various array configurations in a design phase.

The rest of the paper is organized as follows. In Section 2.1, we derive the hybrid scattering-admittance operator of a brick, whereas in Section 2.2 we obtain the functional equations that describe an antenna array. In Section 2.3 we derive the formula for the calculation of the admittance matrix of the array. The numerical solution with the Method of Moments (MoM) and the eigencurrents is the subject of Section 3. Finally, in Section 4, we examine an array of bow-tie antennas to validate the strategy and to discuss the scaling of the total CPU time.

A time dependence in the form of $\exp(j\omega t)$ is implied and suppressed throughout.

2. FORMULATION

We consider an array of N_D antennas made of perfect electric conductor (PEC) immersed in a homogeneous background medium (labelled with ①) and, in accordance with the LEGO philosophy, we enclose each antenna in a brick. In this way, the host medium (labelled with ②) that pads the inside of a brick and the background medium clearly have the same constitutive parameters. The more general case of antennas contained in a dielectric slab can be treated by combining the scattering operator of an interface [13] with the formulas derived in Section 2.1. In the following, we denote the kth brick with $\mathcal{D}_k$, $k = 1, \ldots, N_D$, and the boundary thereof with $\partial\mathcal{D}_k$.

2.1. Hybrid Scattering-Admittance Operator of a Brick

To obtain the hybrid scattering-admittance operator, we start with the electric field integral equation (EFIE) on the surface $\mathcal{S}_o$ of the antenna inside $\mathcal{D}_k$, namely,

$$\left[\mathsf{X}_{oo}\mathbf{J}_o\sqrt{\eta_1} + \mathsf{P}_{ok}\, q_k^i + V_k^g\hat{\boldsymbol{\nu}}\,\delta_{\gamma_o}/\sqrt{\eta_1} \right]_{\tan} = 0, \qquad \text{on } \mathcal{S}_o, \tag{1}$$

where

- $\eta_1 := \sqrt{\mu_1/\varepsilon_1}$ is the intrinsic impedance of medium ① and, here, also of medium ②;
- $\mathsf{X}_{oo}\mathbf{J}_o\sqrt{\eta_1}$ is the normalized secondary electric field produced by $\mathbf{J}_o$, the equivalent electric surface current over $\mathcal{S}_o$; within a normalization factor, X_{oo} denotes the standard EFIE operator on $\mathcal{S}_o$ in a homogeneous infinite space with the properties of medium ① [9, Table II];
- $\mathsf{P}_{ok}\, q_k^i$ is the normalized secondary electric field produced by sources located outside $\mathcal{D}_k$, and q_k^i represents the equivalent surface incident currents on $\partial\mathcal{D}_k$ [9, Eqn. (2)]; P_{ok} is the propagator from $\partial\mathcal{D}_k$ to $\mathcal{S}_o$ [9, Table III].
- $V_k^g\hat{\boldsymbol{\nu}}\delta_{\gamma_o}/\sqrt{\eta_1}$ is the normalized impressed electric field in the delta-gap approximation of the antenna port [10, Eqn. (14)], [15], and V_k^g is the strength of the ideal voltage generator; γ_o is a line on $\mathcal{S}_o$ that defines the antenna port, $\hat{\boldsymbol{\nu}}$ is the unit vector tangential to $\mathcal{S}_o$ and locally perpendicular to γ_o, and δ_{γ_o} denotes a one-dimensional Dirac's distribution localized along γ_o.

Next, we observe that the equivalent surface scattered currents q_k^s on $\partial\mathcal{D}_k$ [9, Eqn. (2)] and the current I_k^a flowing into the antenna port can be written as

$$q_k^s := (\mathsf{P}_{kk}^s)^{-1}\mathsf{P}_{ko}\mathbf{J}_o\sqrt{\eta_1}, \qquad I_k^a := \int_{\gamma_o} \mathrm{d}r\, \hat{\boldsymbol{\nu}} \cdot \mathbf{J}_o(\mathbf{r}) = \int_{\mathcal{S}_o} \mathrm{d}^2r\, \delta_{\gamma_o}\hat{\boldsymbol{\nu}} \cdot \mathbf{J}_o(\mathbf{r}), \tag{2}$$

with the propagators P_{kk}^s and P_{ko} defined in [9, Tables I and III]. Then, formally solving Eq. (1) for $\mathbf{J}_o$ and inserting the result into Eq. (2) yields the relation between incident or impressed quantities and secondary currents, which allows us to identify the desired hybrid scattering-admittance operator of $\mathcal{D}_k$, viz.,

$$\begin{bmatrix} q_k^s \\ \sqrt{\eta_1}I_k^a/l_o \end{bmatrix} = \begin{bmatrix} \mathsf{S}_{kk} & \mathsf{H}_{ko} \\ \mathsf{H}_{ok} & \eta_1\tilde{Y}_{kk} \end{bmatrix} \begin{bmatrix} q_k^i \\ V_k^g/(l_o\sqrt{\eta_1}) \end{bmatrix}, \tag{3}$$

with

$$\mathsf{S}_{kk} := -(\mathsf{P}_{kk}^{\mathrm{s}})^{-1}\mathsf{P}_{k\,\mathrm{o}}\mathsf{X}_{\mathrm{oo}}^{-1}\mathsf{P}_{\mathrm{o}k}, \qquad\qquad \mathsf{H}_{k\mathrm{o}} := -(\mathsf{P}_{kk}^{\mathrm{s}})^{-1}\mathsf{P}_{k\,\mathrm{o}}\mathsf{X}_{\mathrm{oo}}^{-1}(\hat{\boldsymbol{\nu}}\,\delta_{\gamma_{\mathrm{o}}})l_{\mathrm{o}}, \qquad (4)$$

$$\mathsf{H}_{\mathrm{o}k} := -\frac{1}{l_{\mathrm{o}}}\int_{\mathcal{S}_{\mathrm{o}}}\mathrm{d}^2 r\,\hat{\boldsymbol{\nu}}\,\delta_{\gamma_{\mathrm{o}}}\cdot\mathsf{X}_{\mathrm{oo}}^{-1}\mathsf{P}_{\mathrm{o}k}, \qquad\qquad \eta_1\tilde{Y}_{kk} := -\int_{\mathcal{S}_{\mathrm{o}}}\mathrm{d}^2 r\,\hat{\boldsymbol{\nu}}\,\delta_{\gamma_{\mathrm{o}}}\cdot\mathsf{X}_{\mathrm{oo}}^{-1}(\hat{\boldsymbol{\nu}}\,\delta_{\gamma_{\mathrm{o}}}), \qquad (5)$$

where S_{kk} is the usual scattering operator of a passive brick [9, Eqn. (11)], $\tilde{Y}_{kk}$ the input admittance of the array element considered in isolation, and l_{o} the length of γ_{o}. The entries of the hybrid operator in Eqs. (4) and (5) are dimensionless, whereas $q_k^{\mathrm{s,i}}$, $\sqrt{\eta_1}I_k^{\mathrm{a}}/l_{\mathrm{o}}$ and $V_k^{\mathrm{g}}/(l_{\mathrm{o}}\sqrt{\eta_1})$ carry the physical dimension of a power wave per unit length. In the light of Eq. (3) LEGO bricks that contain a single-port antenna can be thought as devices with two ports, namely, a continuously distributed port (the boundary $\partial\mathcal{D}_k$) and a lumped port (the line γ_{o}). The generalization to multi-port antennas inside $\mathcal{D}_k$ is then obvious, but we shall not elaborate this topic any further.

2.2. Combination of Two or More Bricks

In order to model an array comprised of N_D elements (see Fig. 2), we need to combine N_D bricks electromagnetically. This goal is accomplished in the same way as done in [9] by augmenting the incident currents on $\partial\mathcal{D}_k$ in Eq. (3) with the contributions of the scattered currents that flow on the boundaries $\partial\mathcal{D}_n$, $n = 1, \ldots, N_D$, $n \neq k$, of the remaining $N_D - 1$ bricks. In symbols, this reads

$$\begin{bmatrix} q_k^{\mathrm{s}} \\ \sqrt{\eta_1}I_k^{\mathrm{a}}/l_{\mathrm{o}} \end{bmatrix} = \begin{bmatrix} \mathsf{S}_{kk} & \mathsf{H}_{k\mathrm{o}} \\ \mathsf{H}_{\mathrm{o}k} & \eta_1\tilde{Y}_{kk} \end{bmatrix} \begin{bmatrix} q_k^{\mathrm{i}} + \sum_{n\neq k}\mathsf{T}_{kn}\,q_n^{\mathrm{s}} \\ V_k^{\mathrm{g}}/(l_{\mathrm{o}}\sqrt{\eta_1}) \end{bmatrix}, \qquad k = 1, \ldots, N_D, \qquad (6)$$

where T_{kn} is the transfer operator from $\partial\mathcal{D}_n$ to $\partial\mathcal{D}_k$, $n \neq k$ [9, Eqn. (15)]. After a few manipulations the set of $2N_D$ equations represented by Eq. (6) can be cast into a compact form as

$$q^{\mathrm{s}} = \mathsf{S}\,q^{\mathrm{i}} + \frac{1}{l_{\mathrm{o}}\sqrt{\eta_1}}(\mathsf{I} - \mathrm{diag}\,\{\mathsf{S}_{kk}\}\,\mathsf{T})^{-1}\mathrm{diag}\,\{\mathsf{H}_{k\mathrm{o}}\}\,[V^{\mathrm{g}}], \qquad \mathsf{S} := (\mathsf{I} - \mathrm{diag}\,\{\mathsf{S}_{kk}\}\,\mathsf{T})^{-1}\mathrm{diag}\,\{\mathsf{S}_{kk}\}, \qquad (7)$$

$$\frac{\sqrt{\eta_1}}{l_{\mathrm{o}}}\,[I^{\mathrm{a}}] = \mathrm{diag}\,\{\mathsf{H}_{\mathrm{o}k}\}\,(q^{\mathrm{i}} + \mathsf{T}q^{\mathrm{s}}) + \eta_1\mathrm{diag}\,\left\{\tilde{Y}_{kk}\right\}\frac{1}{l_{\mathrm{o}}\sqrt{\eta_1}}\,[V^{\mathrm{g}}], \qquad (8)$$

where

- $q^{\mathrm{s,i}}$ are abstract $N_D \times 1$ vectors with entries $q_k^{\mathrm{s,i}}$ [9, Eqn. (18)], and $[I^{\mathrm{a}}]$, $[V^{\mathrm{g}}]$ are $N_D \times 1$ vectors of antenna port currents (I_k^{a}) and voltages (V_k^{g});
- S is the total scattering operator of the bricks [9, Eqn. (17)], I is a suitable identity operator on the composite surface $\cup_{k=1}^{N_D}\partial\mathcal{D}_k$, and T is the total transfer operator [10, Eqn. (12)], i.e., an abstract $N_D \times N_D$ matrix containing the transfer operators T_{kn};
- the matrix constructor 'diag $\{\circ\}$' builds a diagonal matrix out of the elements it acts on (here, operators and scalars).

The functional Equations (7) and (8) represent the formulation of the array problem with LEGO, and Eq. (7) extends the equations for passive bricks [9, Eqn. (16)]. In transmit mode, when the elements are excited ($[V^{\mathrm{g}}]$ assigned) and there is no external source ($q^{\mathrm{i}} = 0$), the first of Eq. (7) yields q^{s} whereby the radiated fields can be computed. In receive mode, when an impinging EM wave illuminates the array (q^{i} assigned) and the generators are switched off ($[V^{\mathrm{g}}] = 0$), Eq. (8) yields short-circuit currents at the array ports. In fact, the first term in the right-hand side of Eq. (8) can be construed as a current generator, whose strength is determined by the external sources as well as the remaining elements of the array.

2.3. Admittance Matrix of an Antenna Array

The calculation of the $N_D \times N_D$ admittance matrix $[Y]$ of the array requires using Eq. (8) to compute the current I_k^{a} flowing into the kth antenna port when the ith antenna is energized with V_i^{g}, and all the

external sources are switched off ($q_k^{\mathrm{i}} = 0$). Consequently, the entry Y_{ki} of $[Y]$ formally reads

$$Y_{ki} := \left. \frac{I_k^{\mathrm{a}}}{V_i^{\mathrm{g}}} \right|_{\substack{q_k^{\mathrm{i}}=0 \\ V_s^{\mathrm{g}}=0}} = \frac{l_{\mathrm{o}}}{\sqrt{\eta_1} \, V_i^{\mathrm{g}}} \sum_{\substack{n=1 \\ n \neq k}}^{N_D} \mathsf{H}_{\mathrm{o}k} \mathsf{T}_{kn} q_n^{\mathrm{s}} + \tilde{Y}_{kk} \delta_{ki}, \tag{9}$$

with δ_{ki} the Kronecker delta, and $i, s = 1, \ldots, N_D$. As it is apparent from the first of Eq. (7) that q_n^{s} is proportional to V_i^{g} when $q_k^{\mathrm{i}} = 0$, the actual value of V_i^{g} does not enter the formula (9), as expected of a linear system. In fact, we can write Eq. (9) formally as

$$[Y] := \frac{1}{\eta_1} \mathrm{diag}\, \{\mathsf{H}_{\mathrm{o}k}\} \, \mathsf{T}(\mathsf{I} - \mathrm{diag}\, \{\mathsf{S}_{kk}\} \, \mathsf{T})^{-1} \mathrm{diag}\, \{\mathsf{H}_{k\mathrm{o}}\} + \mathrm{diag}\, \left\{\tilde{Y}_{kk}\right\}, \tag{10}$$

on account of Eqs. (7) and (8). It is evident from Eq. (10) that the self-admittance $\tilde{Y}_{kk}$ of an array element in isolation must be augmented with a term that factors in the multiple scattering between the elements.

3. NUMERICAL SOLUTION

3.1. Reduction to a Weak form with the Method of Moments

To evaluate Eqs. (7), (8) and (10) in practice we apply the MoM in the form of Galerkin. Accordingly, we model the surface of bricks and antennas with 3-D triangular tessellations (see Figs. 1(a) and 1(b)), and we expand $q_k^{\mathrm{s,i}}$ ($\mathbf{J}_{\mathrm{o}}$) with sets of $2N_F$ (N_O) Rao-Wilton-Glisson (RWG) basis functions [9]. The standard testing procedure with symmetric L^2 inner products on $\partial \mathcal{D}_k$ and $\mathcal{S}_{\mathrm{o}}$ provides us with the algebraic counterparts of the operators in Eqs. (4) and (5), i.e.,

$$[S_{kk}] := -[P_{kk}^{\mathrm{s}}]^{-1} [P_{k\mathrm{o}}] [X_{\mathrm{oo}}]^{-1} [P_{\mathrm{o}k}], \qquad [H_{k\mathrm{o}}] := -[P_{kk}^{\mathrm{s}}]^{-1} [P_{k\mathrm{o}}] [X_{\mathrm{oo}}]^{-1} [u] \, l_{\mathrm{o}}, \tag{11}$$

$$[H_{\mathrm{o}k}] := -[u]^T [X_{\mathrm{oo}}]^{-1} [P_{\mathrm{o}k}] / l_{\mathrm{o}}, \qquad \eta_1 \tilde{Y}_{kk} := -[u]^T [X_{\mathrm{oo}}]^{-1} [u], \tag{12}$$

where $[u]$ is the $N_O \times 1$ vector with entries

$$u_m := \begin{cases} 0 & \text{if } \gamma_m \notin \gamma_{\mathrm{o}}, \\ l_m & \text{if } \gamma_m \in \gamma_{\mathrm{o}}, \end{cases} \qquad m = 1, \ldots, N_O, \tag{13}$$

with l_m denoting the length of γ_m, the mth (inner) edge of the mesh modelling the antenna surface $\mathcal{S}_{\mathrm{o}}$. Hence, the length of the line γ_{o} introduced in the second of Eq. (2) is computed as $l_{\mathrm{o}} = \sum_m u_m$. It is a simple matter to ascertain that the algebraic operators in Eqs. (11) and (12) are dimensionless. As regards the size of the matrices in Eqs. (11) and (12), $[P_{kk}^{\mathrm{s}}]$ is $2N_F \times 2N_F$, $[X_{\mathrm{oo}}]$ is $N_O \times N_O$, and $[P_{k\mathrm{o}}]$, $[P_{\mathrm{o}k}]$ are $2N_F \times N_O$, $N_O \times 2N_F$, respectively.

With these intermediate results, we can write the weak form of Eqs. (7), (8) and (10) as follows:

$$[q^{\mathrm{s}}] = [S] [q^{\mathrm{i}}] + ([I] - \mathrm{blkdiag}\, \{[S_{kk}]\} [T])^{-1} \mathrm{blkdiag}\, \{[H_{k\mathrm{o}}]\} [V^{\mathrm{g}}] \frac{1}{l_{\mathrm{o}} \sqrt{\eta_1}}, \tag{14}$$

$$[S] := ([I] - \mathrm{blkdiag}\, \{[S_{kk}]\} [T])^{-1} \mathrm{blkdiag}\, \{[S_{kk}]\}, \tag{15}$$

$$[I^{\mathrm{a}}] = \frac{l_{\mathrm{o}}}{\sqrt{\eta_1}} \mathrm{blkdiag}\, \{[H_{\mathrm{o}k}]\} \left([q^{\mathrm{i}}] + [T] [q^{\mathrm{s}}]\right) + \mathrm{diag}\, \left\{\tilde{Y}_{kk}\right\} [V^{\mathrm{g}}], \tag{16}$$

$$[Y] := \frac{1}{\eta_1} \mathrm{blkdiag}\, \{[H_{\mathrm{o}k}]\} [T] ([I] - \mathrm{blkdiag}\, \{[S_{kk}]\} [T])^{-1} \mathrm{blkdiag}\, \{[H_{k\mathrm{o}}]\} + \mathrm{diag}\, \left\{\tilde{Y}_{kk}\right\}, \tag{17}$$

where the matrix constructor 'blkdiag $\{\circ\}$' builds a block diagonal matrix out of the matrices it acts on, $[I]$ is the identity matrix of rank $2N_F N_D$, and $[q^{\mathrm{s,i}}]$ are column vectors containing the $2N_F N_D$ expansion coefficients of $q_k^{\mathrm{s,i}}$.

We conclude this part by commenting on how to choose the LEGO bricks for a model. Size and shape can, in theory, be arbitrary. And yet, the practical choice is somewhat dictated by the geometry of the problem at hand, because the bricks must entirely enclose an array element, nor can they intersect

one another. Provided these constraints are respected, then one should try and minimize the number of unknowns $2N_F$ on a brick's boundary. To this end, making a brick as small as possible would seem logical; however, the mesh ought to be refined to accurately capture the fabric of the near fields around the antenna, and this in turn would cause $2N_F$ to increase. Then again, defining larger bricks makes $2N_F$ increase proportionally, as ever more facets are required to ensure a constant mesh density. Thus, an optimum size and shape for a given problem likely exists, though finding out what that is may not be easy in general. On a related score, in the context of the eigencurrents expansion (Section 3.2) the variation of the rank of $[S_{kk}]$ is discussed in [16] as a function of size and shape of a brick.

3.2. Compression with Eigencurrents Expansion

The actual evaluation of Eqs. (14)–(17) entails filling and inverting $[I] - \text{blkdiag}\{[S_{kk}]\}[T]$, which can be a large matrix even for the analysis of an array with a moderate number of elements. Therefore, we introduce specialized MBFs on the boundaries $\partial \mathcal{D}_k$, and carry out a change of basis so as to compress $[I] - \text{blkdiag}\{[S_{kk}]\}[T]$ and other matrices conformably. This task is accomplished by employing the eigencurrents [9], i.e., the eigenvectors of the algebraic scattering operators $[S_{kk}]$ in Eq. (11).

To begin with, we consider the spectral decomposition of $[S_{kk}]$, namely,

$$[S_{kk}] = [V_{kk}] \operatorname{diag}\left\{\lambda_p^{(k)}\right\}[V_{kk}]^{-1}, \tag{18}$$

with the eigenvalues and relative eigenvectors ordered so that $|\lambda_p^{(k)}| \geq |\lambda_{p+1}^{(k)}|$, $p = 1, \ldots, 2N_F$. Since $[S_{kk}]$ is rank-deficient [16, 17] and, on account of Eq. (18), the weak form of the first of Eq. (6) reads

$$[q_k^{\text{s}}] = [V_{kk}] \operatorname{diag}\left\{\lambda_p^{(k)}\right\}[V_{kk}]^{-1}\left([q_k^{\text{i}}] + \sum_{\substack{n=1 \\ n \neq k}}^{N_D} [T_{kn}][q_n^{\text{s}}]\right) + [H_{k\text{o}}]\frac{V_k^{\text{g}}}{l_{\text{o}}\sqrt{\eta_1}}, \tag{19}$$

we stipulate that only the eigencurrents associated with the first $N_C \leq \min\{2N_F, N_O\}$ eigenvalues contribute to the multiple scattering among the bricks and must be employed to represent $[q_k^{\text{s}}]$.

Next, we form the matrices $[V_C^{(k)}]$ ($[U_C^{(k)}]$) with the first N_C columns (rows) of $[V_{kk}]$, ($[V_{kk}]^{-1}$), and we also define the following block-diagonal matrices

$$[V_C] := \text{blkdiag}\left\{[V_C^{(k)}]\right\}, \qquad [U_C] := \text{blkdiag}\left\{[U_C^{(k)}]\right\}, \tag{20}$$

then by definition

$$[U_C][V_C] = [I_C], \tag{21}$$

where $[I_C]$ is the identity matrix of rank $N_D N_C$. With these positions, we have

$$[q^{\text{s}}] = [V_C][\tilde{q}^{\text{s}}], \qquad \text{blkdiag}\{[S_{kk}]\} = [V_C][\Lambda_C][U_C], \tag{22}$$

where $[\Lambda_C] = \text{blkdiag}\left\{\operatorname{diag}\left\{\lambda_p^{(k)}\right\}\right\}$, $p = 1, \ldots, N_C$. To proceed, by taking advantage of Eq. (15), we rewrite Eq. (14) as follows

$$([I] - \text{blkdiag}\{[S_{kk}]\}[T])[q^{\text{s}}] = \text{blkdiag}\{[S_{kk}]\}[q^{\text{i}}] + \text{blkdiag}\{[H_{k\text{o}}]\}[V^{\text{g}}]\frac{1}{l_{\text{o}}\sqrt{\eta_1}}, \tag{23}$$

and then as

$$([I] - [V_C][\Lambda_C][U_C][T])[V_C][\tilde{q}^{\text{s}}] = [V_C][\Lambda_C][U_C][q^{\text{i}}] + \text{blkdiag}\{[H_{k\text{o}}]\}[V^{\text{g}}]\frac{1}{l_{\text{o}}\sqrt{\eta_1}}, \tag{24}$$

on account of Eq. (22). By left multiplying by $[U_C]$ we find, in view of Eq. (21),

$$([I_C] - [\Lambda_C][U_C][T])[V_C][\tilde{q}^{\text{s}}] = [\Lambda_C][U_C][q^{\text{i}}] + [U_C]\text{blkdiag}\{[H_{k\text{o}}]\}[V^{\text{g}}]\frac{1}{l_{\text{o}}\sqrt{\eta_1}}, \tag{25}$$

in which the matrix in the left-hand side has now rank $N_C N_D \ll 2N_F N_D$. Formally inverting Eq. (25) and reverting back to the original sets of basis functions leads to

$$[S] := [V_C]([I_C] - [\Lambda_C][U_C][T])^{-1}[\Lambda_C][U_C], \tag{26}$$

$$[q^{\mathrm{s}}] = [S][q^{\mathrm{i}}] + [V_C]([I_C] - [\Lambda_C][U_C][T])^{-1}[U_C]\,\mathrm{blkdiag}\,\{[H_{k\mathrm{o}}]\}[V^{\mathrm{g}}]\frac{1}{l_{\mathrm{o}}\sqrt{\eta_1}}. \tag{27}$$

In like manner, to evaluate the admittance matrix $[Y]$ through Eq. (17), we consider the expression

$$[Y] := \frac{1}{\eta_1}\mathrm{blkdiag}\,\{[H_{\mathrm{o}k}]\}[T][V_C]([I_C] - [\Lambda_C][U_C][T][V_C])^{-1}[U_C]\,\mathrm{blkdiag}\,\{[H_{k\mathrm{o}}]\} + \mathrm{diag}\,\{\tilde{Y}_{kk}\}, \tag{28}$$

which is based on Eq. (27) with $[q^{\mathrm{i}}] = 0$.

From a numerical standpoint, to avoid storing and inverting large matrices, we proceed as follows:

- To fill the matrix $[I_C] - [\Lambda_C][U_C][T][V_C]$ we evaluate matrices of the form $[\Lambda_C^{(k)}][U_C^{(k)}][T_{kn}][V_C^{(n)}]$ by examining two bricks at a time; more importantly, the inversion of $[I_C] - [\Lambda_C][U_C][T][V_C]$ can be done through LU factorization.
- To fill the matrix $\mathrm{blkdiag}\,\{[H_{\mathrm{o}k}]\}[T][V_C]$, which is size $N_D \times N_D N_C$, we compute "small" matrices $[H_{\mathrm{o}k}][T_{kn}][V_C^{(n)}]$.
- To fill $[U_C]\,\mathrm{blkdiag}\,\{[H_{k\mathrm{o}}]\}$, which is size $N_C N_D \times N_D$ and block-diagonal, we only need compute and store the N_D column vectors $[U_C^{(k)}][H_{k\mathrm{o}}]$.
- To determine $[q^{\mathrm{s}}]$ we first compute the scattered currents coefficients $[\tilde{q}^{\mathrm{s}}]$ in the eigencurrents basis from Eq. (25), and then we revert to the original basis by virtue of Eq. (22); in this way, the actual calculation of $[S]$ in Eq. (26) is avoided.

4. NUMERICAL EXAMPLE

The extended LEGO described in the previous sections, along with the numerical solution with the MoM and the compression with the eigencurrents, has been implemented in a FORTRAN code (cf. [14]). The latter can solve disconnected antenna arrays by combining LEGO bricks which contain a single-port PEC antenna with arbitrary shape. To discuss the performance of the code, we present selected simulation results for planar arrays comprised of bow-tie antennas in free space.

The triangular tessellation of a bow-tie and the dimensions thereof are presented in Fig. 1(a), whereas the mesh of the cuboidal brick which encloses a bow-tie is pictured in Fig. 1(b); the dimensions of a brick are $15 \times 15 \times 10.5$ mm. For the numerical solution (Section 3.1), we introduce $N_O = 232$ RWG functions on a bow-tie antenna and $2N_F = 2592$ RWG functions on a brick. By using the LEGO brick as a building block, we can easily solve antenna arrays of different shape and size by computing the hybrid scattering-admittance operator (Section 2.1) *only once* for a given operational frequency.
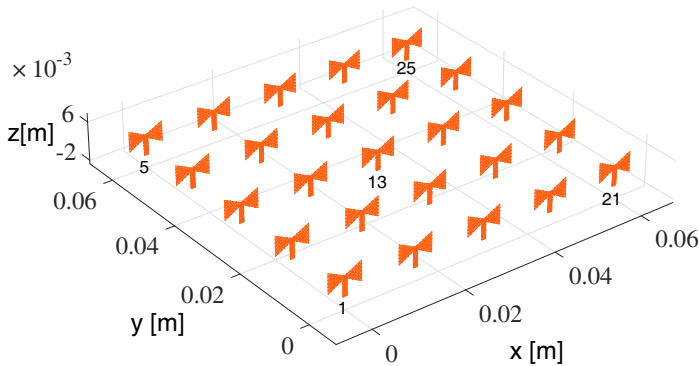

Figure 2. LEGO for antenna arrays: a planar regular arrangement of 5×5 bow-tie antennas (Fig. 1(a)); the separation along both lattice directions is 15 mm.
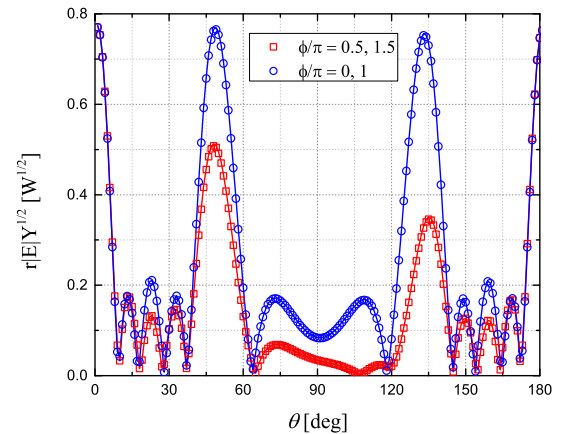

Figure 3. LEGO for antenna arrays: radiated electric field of the array in Fig. 2 at $f = 27$ GHz versus the elevation angle; ($\Box$), ($\circ$) LEGO method, ($-$) reference.

For instance, shown in Fig. 2 is a realization comprised of $N_D = 5 \times 5 = 25$ elements arranged in a square lattice. The array sits in the xOy plane and the separation of the antenna elements along both directions is 15 mm. Correspondingly, the total size of the matrix $[I] - \text{blkdiag}\{[S_{kk}]\}[T]$ appearing in (15) and (17) is $2N_F N_D = 2592 \times 25 = 64800$. Thanks to the eigencurrents expansion with $N_C = 150$ eigencurrents per brick the rank of the compressed matrix in Eqs. (26) and (28) becomes $N_C N_D = 3750$. This case study shall also serve as an example of validation for the overall approach; the pertinent reference results have been obtained by solving a standard EFIE over the total surface of the antennas to compute the electric surface current density induced thereon, and the size of the system for such computation is $N_O N_D = 232 \times 25 = 5800$.

We have analyzed the array of Fig. 2 in the frequency range $f \in [10, 35]$ GHz. Plotted in Fig. 3 is the normalized electric field radiated by the array in the principal planes at $f = 27$ GHz, when all the elements are energized with $V_k^\text{g} = 1$ V and the external sources are switched off (see Eq. (14)); the reference solutions have been drawn as solid lines. At this frequency the inter-element separation is about 1.35 times the wavelength in free space, and the array exhibits two full and two partial grating lobes. The impedance matrix $[Z]$ of the array can be obtained by inverting $[Y]$ computed through Eq. (28). The behaviour of selected self- and trans-impedances versus f is plotted in Fig. 4 where, again, the continuous lines represent the reference solution; as can be seen, the elements resonate at $f = 27$.
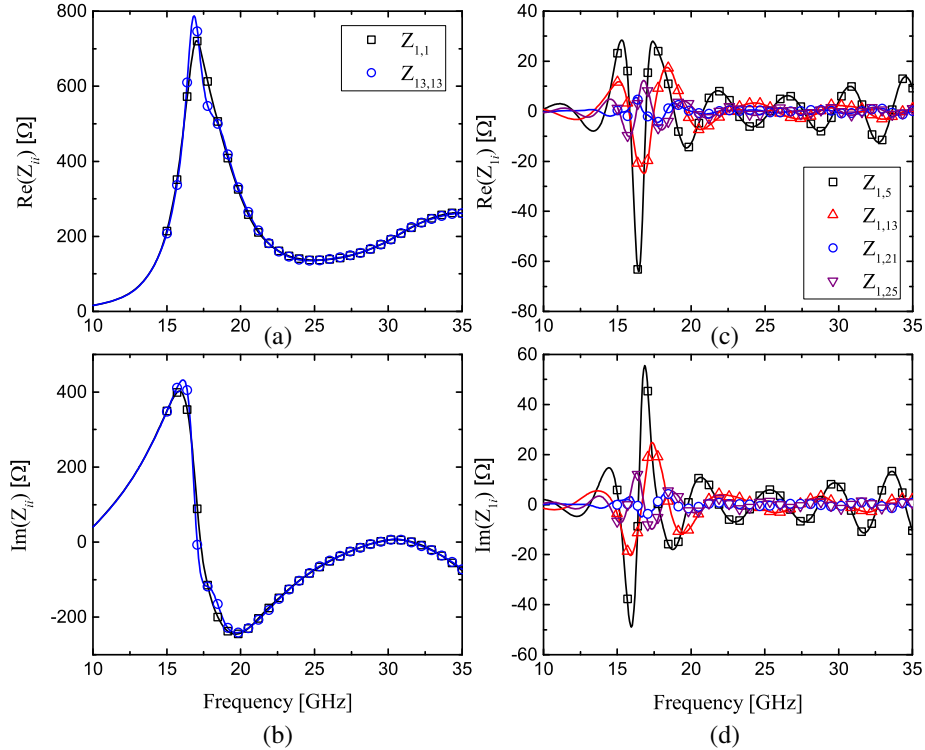

Figure 4. LEGO for antenna arrays: (a), (b) real and imaginary parts of the self-impedance versus frequency for elements 1 and 13 in Fig. 2; (c), (d) real and imaginary parts of trans-impedance versus frequency for elements indicated in Fig. 2; ($\square$), ($\circ$), ($\triangle$), ($\triangledown$) LEGO method, ($-$) reference.

All in all, the excellent agreement between the reference solution and the results obtained through Eqs. (27) and (28) validates the LEGO approach as well as the compression with the eigencurrents.

Next, we have investigated how the CPU time scales with the size of the problem, i.e., the number of bricks N_D. To this purpose, we have solved planar arrays comprised of increasing numbers of bow-ties (Fig. 1(a)). However, we have modelled the boundary of the enclosing bricks with a coarser mesh, and also employed fewer eigencurrents in Eqs. (27) and (28). This expedient allows us to speed up the solution process and still to highlight patterns, if any, of the overall CPU time as a function of N_D.

To be specific, we have introduced $N_O = 232$ RWG functions over each antenna and $2N_F = 1152$ over each brick, and we have chosen $N_C = 10$ eigencurrents for the compression. The calculations have been carried out on a 64-bit Windows-based system with an Intel Core i7 3.4-GHz processor and 16 GB RAM.

The CPU times are listed in Table 1 in correlation with various characteristic sizes of the problem, including the number of transfer matrices $[T_{nk}]$ $N_D(N_D - 1)$, the total number of unknowns $2N_F N_D$, and the total number of eigencurrents $N_C N_D$. The role of the eigencurrents in reducing the size of the problem becomes especially manifest, if we compare the rank $(2N_D N_F)$ of the original scattering matrix with the rank $(N_D N_C)$ of the deflated one. Additional insight can be gained from Fig. 5, which plots the CPU time required to solve the arrays as a function of N_D. Apparently, the overall CPU time grows only linearly, even though the number of transfer matrices grows as $\mathcal{O}(N_D^2)$. Such behavior is a consequence of having exploited the translational symmetry of the problem, which causes the occurrence of sub-sets of identical transfer matrices. Since only one transfer matrix per sub-set has actually to be computed, the total number of transfer matrices effectively scales as $\mathcal{O}(N_D)$ (cf. [9, 18]).

Table 1. CPU times vs characteristic sizes of the LEGO model.

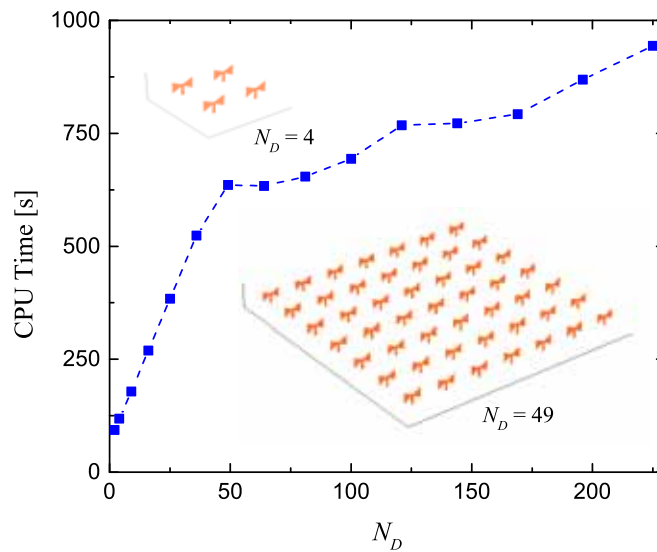| N_D	$N_D(N_D - 1)$	$2N_F N_D$	$N_C N_D$	Time [s]
4	12	4608	40	118
25	600	28800	250	384
49	2352	56448	490	636
81	6480	93312	810	654
100	9900	115200	1000	694
121	14520	139392	1210	768
144	20592	165888	1440	772
169	28392	194688	1690	792
196	38220	225792	1960	869
225	50400	259200	2250	944

Figure 5. LEGO for antenna arrays: CPU time vs number of bricks (for visualization's sake the markers are joined with a dashed line). Insets: two realizations of the array.

5. CONCLUSION AND OUTLOOK

We have proposed an extension of the LEGO method for the analysis of disconnected PEC antennas in a homogeneous background medium. The newly derived functional equations Eq. (7) allow fitting general array problems within a unified framework. With the aid of a numerical example, we have shown that the formulation based on scattering-admittance operators is viable, efficient and yields the same results as the direct solution of a suitable EFIE with the baseline MoM. At a first glance, defining bricks and computing scattering-admittance operators may seem an unnecessary complication vis-à-vis a direct approach in tandem with MBFs. And yet, LEGO bricks can provide better conditioning and versatility: the former, because the mesh over a brick's surface can be made uniform, the latter, because the bricks can be re-used and combined arbitrarily to a large extent. For instance, a simplified preliminary design of a complicated antenna array with LEGO turns out handy for the optimization of position and number of elements in a sparse array configuration.

Computing the radiated fields is no different than determining the scattered fields in the standard LEGO [9], and it essentially requires the Fourier transform of the currents q_k^{s} which are given as the linear combination of $2N_F$ RWG functions on $\partial\mathcal{D}_k$. Even though the total number of unknowns is $2N_F N_D$, we need only compute the Fourier transform of N_F RWG functions, because a) electric and magnetic currents on $\partial\mathcal{D}_k$ are expanded on the same set [9, Section IV.B], and b) the Fourier transforms of shifted RWG functions defined on different bricks differ solely for a phase factor. Thus, the relevant computation time is determined by N_F plus an overhead for the linear combination which, of course, does change with N_D. We observe that, since the number of eigencurrents $N_C \ll 2N_F$, it may be worth expressing the far fields as a combination of the fields radiated by each eigencurrent. Other techniques, such as hybridization of uniform geometrical theory of diffraction and MoM [19], or the adaptive cross approximation [20] could also be applied to LEGO starting with the currents q_k^{s} on $\partial\mathcal{D}_k$.

ACKNOWLEDGMENT

REFERENCES

1. Holter, H. and H. Steyskal, "On the size requirement for finite phased-array models," *IEEE Transactions on Antennas and Propagation*, Vol. 50, 836–840, Jun. 2002.

2. Jorgenson, R. E. and R. Mittra, "Efficient calculation of the free-space periodic Green's function," *IEEE Transactions on Antennas and Propagation*, Vol. 38, 633–642, May 1990.

3. Skrivervik, A. K. and J. R. Mosig, "Analysis of printed array antennas," *IEEE Transactions on Antennas and Propagation*, Vol. 45, 1411–1418, Sept. 1997.

4. Zhang, B., G. Xiao, J. Mao, and Y. Wang, "Analyzing large-scale non-periodic arrays with synthetic basis functions," *IEEE Trans. Antennas Propag.*, Vol. 58, 3576–3584, Nov. 2010.

5. Maaskant, R., R. Mittra, and A. G. Tijhuis, "Fast analysis of large antenna arrays using the characteristic basis function method and the adaptive cross approximation algorithm," *IEEE Trans. Antennas Propag.*, Vol. 56, 3440–3451, Nov. 2008.

6. Bekers, D. J., S. J. L. van Eijndhoven, and A. G. Tijhuis, "An eigencurrent approach for the analysis of finite antenna arrays," *IEEE Trans. Antennas Propag.*, Vol. 58, 3772–3782, Dec. 2009.

7. Li, M. K. and W. C. Chew, "Wave-field interaction with complex structures using equivalence principle algorithm," *IEEE Trans. Antennas Propag.*, Vol. 55, 130–138, Jan. 2007.

8. Van de Water, A. M., B. P. de Hon, M. C. van Beurden, A. G. Tijhuis, and P. de Maagt, "Linear embedding via Green's operators: A modeling technique for finite electromagnetic band-gap structures," *Physics Review E*, Vol. 72, 1–11, Nov. 2005.

9. Lancellotti, V., B. P. de Hon, and A. G. Tijhuis, "An eigencurrent approach to the analysis of electrically large 3-D structures using linear embedding via Green's operators," *IEEE Trans. Antennas Propag.*, Vol. 57, 3575–3585, Nov. 2009.

10. Lancellotti, V. and D. Melazzi, "Hybrid LEGO-EFIE method applied to antenna problems comprised of anisotropic media," *Forum in Electromagnetic Research Methods and Application Technologies (FERMAT)*, Vol. 6, 1–19, 2014, Online at www.e-fermat.org.

11. Olvera, A. D. J. F., D. Melazzi, and V. Lancellotti, "Beam-forming and beam-steering capabilities of a reconfigurable plasma antenna array," *Progress In Electromagnetics Research C*, Vol. 65, 11–22, 2016.

12. Lancellotti, V. and A. G. Tijhuis, "Solving wave propagation within finite-sized composite media with linear embedding via Green's operators," *Progress In Electromagnetics Research M*, Vol. 25, 127–140, 2012.

13. Lancellotti, V., B. P. de Hon, and A. G. Tijhuis, "Scattering from large 3-D piecewise homogeneous bodies through linear embedding via Green's operators and Arnoldi basis functions," *Progress In Electromagnetics Research*, Vol. 103, 305–322, 2010.

14. Mokhlespour, S., V. Lancellotti, and A. G. Tijhuis, "Hybrid scattering-admittance operators for the analysis of finite antenna arrays," *9th European Conference on Antennas and Propagation (EuCAP 2015)*, 1–4, May 2015.

15. Balanis, C. A., *Antenna Theory: Analysis and Design*, 2nd Edition, John Wiley & Sons, Inc., New York, 1997.

16. Lancellotti, V., B. P. de Hon, and A. G. Tijhuis, "On the convergence of the eigencurrent expansion method applied to linear embedding via Green's operators (LEGO)," *IEEE Trans. Antennas Propag.*, Vol. 58, 3231–3238, Oct. 2010.

17. Lancellotti, V. and R. Maaskant, "A comparison of two types of macro basis functions defined on LEGO electromagnetic bricks," *9th European Conference on Antennas and Propagation (EuCAP 2015)*, (Lisbon, Portugal), Apr. 2015.

18. Lancellotti V. and A. G. Tijhuis, "Linear embedding via Green's operators," *Computational Electromagnetics*, R. Mittra (ed.), 227–257, Springer Science + Business Media, New York, 2014.

19. Çivi, O. A., P. H. Pathak, H.-T. Chou, and P. Nepa, "A hybrid uniform geometrical theory of diffraction-moment method for efficient analysis of electromagnetic radiation/scattering from large finite planar arrays," *Radio Science*, Vol. 35, No. 2, 607–620, 2000.

20. Maaskant, R. and V. Lancellotti, "Field computations through the ACA algorithm," *9th European Conference on Antennas and Propagation (EuCAP 2015)*, Lisbon, Portugal, Apr. 2015.